Research Square

Preprints are preliminary reports that have not undergone peer review.
They should not be considered conclusive, used to inform clinical practice,
or referenced by the media as validated information.

A Reduced-Component Serum-Free Medium Supports Rapid Adipogenic Differentiation of Bovine Adipose-Derived Stem Cells under Serum-free Conditions

Ye Rim Kim
Jeonbuk National University
Si Won Jang
Jeonbuk National University
Jae Ho Han
Jeonbuk National University
Ga Rim Na
Jeonbuk National University
Ji Hoon Park
Jeonbuk National University
Seung Moon Park
Jeonbuk National Universityk
Min-Ho Lee
Jeonbuk National University
Hyun Woo Choi
choihw@jbnu.ac.kr
Jeonbuk National University

Article

Keywords: cultivated fat, tissue engineering, lipid accumulation, adipose-derived progenitor cells, recombinant albumin, serum-free adipogenesis

Posted Date: October 7th, 2026

DOI: https://doi.org/10.21203/rs.3.rs-10696095/v1

License: This work is licensed under a Creative Commons Attribution 4.0 International License.
Read Full License

Additional Declarations: No competing interests reported.

Abstract

Simultaneous muscle and adipose tissue formation is a key strategy for cultured meat production. While myogenic differentiation occurs within days, adipogenic differentiation remains relatively slow and inefficient, constraining co-differentiation. Here, we developed an albumin-based reduced-component defined medium (AdB5), consisting of albumin, basic fibroblast growth factor, L-ascorbic acid, insulin, and rosiglitazone, that supports rapid adipogenic differentiation of bovine adipose-derived stem cells under serum-free conditions. AdB5 induced lipid accumulation as early as day 2 with an approximately 65.1-fold increase in Oil Red O-positive area on day 10 compared with conventional serum-based conditions. Transcriptomic analysis revealed early changes in adipogenesis-associated genes, including CEBPB and CEBPD, with fatty acid metabolism enrichment and extracellular matrix remodeling on day 2. AdB5 medium also supported adipogenic and myogenic differentiation in mixed bovine adipose- and muscle-derived stem cell cultures and three-dimensional adipose-muscle construct formation under a single differentiation condition.

INTRODUCTION

'Cultured' meat is emerging as a promising alternative for the production of edible animal tissues using cell culture technologies [1–3]. Although skeletal muscle engineering has advanced substantially, adipose tissue remains comparatively underexplored despite its critical role in meat flavor, texture, juiciness, and overall sensory characteristics [4–8].

Cultured meat production requires coordinated muscle and adipose tissue formation [9]. However, while myogenic differentiation occurs within a few days, adipogenic differentiation of bovine cells typically requires more than 15–20 days, resulting in a temporal mismatch that limits co-differentiation. Additionally, adipogenic differentiation remains relatively slow and often relies on complex induction conditions, presenting a challenge for coordinated muscle-adipose tissue formation.

A serum-free and chemically defined culture system is important for the development of controlled and reproducible cultured meat production. However, fetal bovine serum (FBS) use introduces high costs, batch-to-batch variability, and ethical concerns [10,11]. Adipogenic differentiation typically relies on complex induction cocktails, including insulin (INS), dexamethasone (DEX), 3-isobutyl-1-methylxanthine (IBMX), rosiglitazone (ROSI), and indomethacin (IND) [4,7,10], which increase formulation complexity and may present challenges for food applications [12,13].

Serum-free or defined culture systems for muscle stem cells (MuSCs) enable controlled proliferation and myogenic differentiation [14–19]. Particularly, albumin-based defined media supports bovine MuSC (bMuSC) growth and myogenic differentiation, even in the absence of additional growth factors [11,20]. In contrast, serum-free adipogenic differentiation systems remain limited, particularly in livestock-derived cells, and defined conditions for efficient adipocyte formation are not well established [21–23].

Furthermore, the incomplete disclosure of medium composition in some prior studies limits reproducibility and comparison across studies.

In this study, we developed an albumin-based reduced-component defined medium (AdB5) consisting of albumin, basic fibroblast growth factor (bFGF), L-ascorbic acid, ROSI, and INS, which supports rapid adipogenic differentiation of bovine adipose-derived stem cells (bADSCs) under serum-free conditions. AdB5 induced lipid accumulation on day 2, with an ORO-positive area up to 65.1-fold higher than that under the FBS-based differentiation condition on day 10. Transcriptomic analysis showed early changes in adipogenic-associated genes, including *CEBPB* and *CEBPD*, together with enrichment of pathways related to fatty acid metabolism and extracellular matrix remodeling. AdB5 also supported adipogenic and myogenic differentiation in mixed bADSC-bMuSC cultures and 3D adipose-muscle construct formation.

MATERIALS AND METHODS

Animal experiments

This study followed the recommendations of the ARRIVE guidelines. All animal procedures were approved by the Animal Ethics Committee of Jeonbuk National University (JBNU; NON2023-137-005), Republic of Korea. All experiments were performed in accordance with the ethical guidelines and regulations of Jeonbuk National University.

bADSC isolation and culture

Primary bADSCs were isolated from subcutaneous adipose tissue obtained from Korean native cattle and transported to the laboratory on ice at 4 ℃. Adipose tissues were rinsed with 75% ethanol, washed with phosphate-buffered saline (PBS; 10010-072, Gibco) containing antibiotic–antimycotic solution (A/A; 15240-112, Gibco), minced into small fragments, and enzymatically digested in α-MEM (12571-063, Gibco) supplemented with collagenase type Ⅱ (CLS-2, Worthington) at 37 ℃ for 2 h with intermittent vortex mixing. The digestion was neutralized with α-MEM containing FBS (26140-079, Gibco), and resulting cell suspension was sequentially filtered through 100 μm (93100, SPL) and 70 μm strainers (93070, SPL). The cells were collected by centrifugation (440 ×g, 5 min, 4 ℃), treated with red blood cell lysis buffer (R7757, Sigma-Aldrich), and resuspended in bADSC growth medium (bADSC-GM; Table S1). The cells were seeded on culture dishes coated with 0.1% gelatin (G1319, Sigma-Aldrich) and maintained at 37 ℃ in a humidified incubator with 5% CO_2. Primocin (ant-pm-2, InvivoGen) was added only during the initial 6 days. For long-term storage, the cells were cryopreserved in FBS containing 10% dimethyl sulfoxide (D2650, Sigma-Aldrich) and stored in liquid nitrogen

bMuSC isolation and culture

bMuSCs were isolated and cultured using the same procedure as described for bADSCs, except for the digestion medium composition. Briefly, bovine skeletal muscle tissues were minced and enzymatically digested in DMEM/F12 (11320-082, Gibco) supplemented with 0.25% trypsin–EDTA (25200-072, Gibco), collagenase type Ⅱ, and Dispase II (4942078001, Roche) for 30 min at 37°C. The resulting cells were seeded on 0.1% gelatin-coated culture dishes and maintained in bovine satellite cell growth medium (bMuSC-GM).

bADSC culture and differentiation

Passage 4 bADSCs (1.2×10^4 cell/cm^2) were seeded on 0.1% gelatin-coated culture dishes containing bADSC-GM and incubated at 37 ℃ in a humidified atmosphere with 5% CO_2. The culture medium was replaced every 2 days. When the cells reached 85–95% confluence, the growth medium was replaced with differentiation medium (3% FBS and AdB5). The differentiation medium was refreshed every 2 days throughout the differentiation period.

Media optimization during adipogenic differentiation

Adipogenic differentiation cocktail composition optimization

To optimize the adipogenic differentiation cocktail, the cells were incubated in a constant basal medium supplemented with various combinations of adipogenic supplements. Each cocktail formulation was applied for the indicated differentiation period, and adipogenic differentiation efficiency was assessed using lipid accumulation assays and adipogenic marker gene expression. These results were used to identify the optimal combination of supplements to promote robust adipogenic differentiation.

Component-dropout assay for medium optimization

To identify the reduced-component adipogenic differentiation cocktail, component-dropout experiments were conducted. Individual supplements were reduced to 50% of their original concentrations or completely omitted from the optimized differentiation medium while maintaining all other components. Adipogenic differentiation was assessed by lipid staining and gene expression analysis, and the results were used to refine the composition of the final reduced-component differentiation medium.

bADSC–bMuSC co-differentiation

bADSCs and bMuSCs at passage 4 were simultaneously seeded on 0.1% gelatin-coated culture dishes at a constant total density of 1.2×10^4 cell/cm^2, while varying the bADSC:bMuSC ratios (0:10, 1:9, 3:7, 5:5, 7:3, 9:1, 10:0). During the proliferation phase, co-cultures were maintained in bADSC-GM at 37 ℃ in a

humidified incubator with 5% CO_2, and the medium was refreshed every 2 days. When the cultures reached approximately 85–95% confluence, the growth medium was replaced with AdB5 differentiation medium.

Immunofluorescent staining

Immunocytochemical analysis was performed to assess the phenotype of differentiated cells in each medium. The cells were fixed with 4% paraformaldehyde (PC-2031-050-00; Biosesang) for 30 min at room temperature (RT) and washed thrice with PBS. The fixed cells were permeabilized and blocked with 0.3% Triton X-100 and 3% bovine serum albumin (BSA; Bovostar, Bovogen) in PBS for 2 h at RT and incubated overnight at 4 ℃ with a primary antibody against MyHC (MF20, 1:20; Developmental Studies Hybridoma Bank). After washing thrice with PBS containing 0.3% Triton X-100, the cells were incubated with an Alexa 568-conjugated anti-mouse secondary antibody (A11004, Invitrogen) for 2 h at RT. To visualize the lipid droplets, the cells were subsequently stained with 10 μM BODIPY (D3922, Sigma-Aldrich) for 10 min at RT. Nuclear counterstaining was performed with 4'-6-diamidino-2-phenylindole (DAPI; 1 μg mL^{-1}) for 10 min, followed by three washes with PBS. Fluorescent images were acquired using a Leica DMi8 microscope and confocal laser-scanning microscope (LSM 880 with Airyscan; Carl Zeiss, Germany) installed at the Center for University-wide Research Facilities (CURF) at Jeonbuk National University.

Fusion index analysis

Myogenic differentiation was quantitatively assessed by calculating the fusion index from the MyHC-stained images. The fusion index was defined as the percentage of nuclei within MyHC-positive multinucleated myotubes (containing ≥ 2 nuclei) relative to the total number of nuclei. At least 10 random fields were analyzed for each condition, and the average fusion index was calculated for each experimental group.

ORO staining

Liquid accumulation was assessed by ORO staining. The cells were then gently rinsed twice with PBS and fixed in 4% paraformaldehyde for 10 min at RT. After fixation, the cells were washed twice with distilled water (DW) and preincubated with 60% (v/v) 2-propanol for 5 min at RT to reduce background lipid staining. Following removal of 2-propanol, the samples were air-dried completely and incubated with 60% ORO working solution (300 μL per well) (O1391, Sigma-Aldrich) for 30 min at RT. Excess stain was removed by repeated washing with DW until the background was clear. The cells were then covered with PBS (300 μL per well) and imaged under a light microscope.

For the quantitative analysis of lipid accumulation, ORO-stained images were captured using a bright-field microscope under identical imaging settings. Lipid accumulation was quantified using the ImageJ software (National Institutes of Health, USA). Briefly, the images were converted to 8-bit grayscale and a consistent threshold was applied across all samples to identify the ORO-positive areas, which were measured and normalized to the total image area for comparative analysis.

GelMA cryogel preparation and cell differentiation

GelMA was synthesized according to previously reported methods [24,25], with minor modifications. Briefly, 10% (w/w) gelatin powder was dissolved in DPBS in a water bath at 50 ℃. Methacrylic anhydride (8% v/v) was gradually added to the gelatin solution with continuous stirring and allowed to react for 3 h. The reaction was terminated by adding 5× DPBS. The resulting solution was transferred into dialysis bags and dialyzed against deionized water for 10 days; the water was changed daily. After dialysis, the solution was freeze-dried to obtain GelMA for long-term storage.

For the GelMA-based cryogels, 20 mg mL^{-1} GelMA was fully dissolved in DW. TEMED (7% w/v) was added, and the mixture was incubated at − 4 ℃ for 20 min. Subsequently, APS (14% w/v) was added at a TEMED-to-APS ratio of 1:6. After thorough mixing, the solution was poured into molds (48-well plate) and frozen at − 80 ℃ overnight, followed by freeze-drying to obtain cryogel scaffolds.

For cell differentiation, bADSC and bMuSCs were cultured on the GelMA scaffolds. Cells were seeded at a density of 1×10^6 per scaffold and maintained in bADSC-GM for 4 days, followed by incubation in AdB5 differentiation medium for 10 days. The medium was changed every two days with gentle handling to avoid structural damage.

Scanning electron microscopy

The samples were fixed in a solution containing 2% formaldehyde, 2.5% glutaraldehyde (G5882, Sigma-Aldrich), and 0.1 M cacodylate buffer (C0250, Sigma-Aldrich) for 24 h, rinsed with 0.1 M cacodylate buffer, dehydrated through a graded ethanol series, and dried using hexamethyldisilazane (440191, Sigma-Aldrich). The samples were then sputter-coated with a thin layer of gold using a sputter coater (SC7620 Mini Sputter Coater, Quorum Technologies) before imaging using a scanning electron microscope (JSM-IT200, JEOL).

RT-qPCR

Cell lysates were collected after removing the culture medium and washing with PBS. The cells were detached using 0.25% trypsin–EDTA and pelleted by centrifugation (440 ×g, 5 min, 4 ℃). Total RNA was isolated using the AccuPrep® Universal RNA Extraction Kit (K-3141, Bioneer) according to the manufacturer's instructions. For cDNA synthesis, 1 μg total RNA was reverse-transcribed using the Accupower® CycleScript RT Premix (K-2047-B, Bioneer) following the manufacturer's instructions. Quantitative real-time PCR (RT-qPCR) was performed using PowerupTM SYBR Green Master Mix (A25918, Applied Biosystems) with the primer pairs listed in Table S2. The cycle threshold (CT) values were obtained from three replicates. Relative gene expression levels were calculated using the $2^{-\Delta\Delta CT}$ method with GAPDH as the internal control. Statistical significance between groups was evaluated using the Student's t-test relative to the respective controls.

RNA sequencing

Library preparation and sequencing

Total RNA was extracted from harvested samples using AccuPrep® Universal RNA Extraction Kit according to the manufacturer's instructions. Sequencing libraries were prepared from the total RNA samples using an Illumina strand-specific library preparation kit and sequenced on an Illumina platform to generate paired-end reads. RNA sequencing and primary data processing were performed by a commercial service provider (LAS Co., Ltd., South Korea).

Read alignment and quantification

Raw sequencing reads were assessed for quality using FastQC (v0.11.5). Adapter sequences and low-quality bases were trimmed using Skewer (v0.2.2). Cleaned reads were aligned to the *Bos Taurus* reference genome ARS-UCD1.2 (UCSC) using the STAR aligner (v2.6) with default parameters and the option outFilterIntronMotifs RemoveNoncanonicalUnannotated. As the libraries were prepared strand-specifically, strand information was preserved using the library-type fr-first strand option. Gene expression levels were quantified using Cuffquant from the CuffLinks package (v2.2.1), with the masking of ribosomal and transfer RNA genes (rRNA.tRNA.gtf), fragment bias correction (frag-bias-correct genome.fa), and multi-read correction (multi-read-correct). Expression values were calculated as fragments per kilobase of transcript per million mapped reads (FPKM) based on gene models obtained from the UCSC genome browser.

Quality control and normalization

Normalized expression matrices were generated using Cuffnorm from the CuffLinks package. Genes with low read coverage were excluded from the downstream analyses. Normalized FPKM values were used for subsequent statistical analyses and visualization.

Dimensionality reduction and differential expression analysis

Differential expression analysis between the experimental conditions was performed using Cuffdiff from the CuffLinks package with default parameters and the strand-specific option library-type fr-firststrand. Genes with a fold change ≥ 2 and a false discovery rate (FDR, q-value) ≤ 0.05 were considered significantly differentially expressed. Hierarchical clustering and principal component-based visualization were performed using normalized FPKM values, and the results were visualized as heat maps using R software (v4.5.2).

Gene ontology analysis

Overrepresented functional categories were identified using the g:Profiler2 R package (v0.2.0) based on Gene Ontology (GO) terms and KEGG pathways. Functional enrichment analyses were performed separately for upregulated and downregulated gene sets. Adjusted p-values were calculated using the g:SCS multiple testing correction method, and terms with adjusted p-value < 0.05 were considered statistically significant.

Statistical analysis

Sample replicates consisted of cells derived from the same donor animal and cultured in separate vessels. Data from independent experiments were pooled and expressed as mean ± standard error of the mean (SEM). Statistical analyses were performed using the R software. Comparisons between two groups were conducted using Student's t-test, whereas multiple-group comparisons were analyzed using one-way analysis of variance (ANOVA), followed by Dunnett's multiple-comparison test against the respective controls. A p-value < 0.05 was considered statistically significant.

RESULTS

Albumin supports rapid adipogenic differentiation in bovine adipose-derived stem cells

Albumin supplementation supports the proliferation and myogenic differentiation of bMuSCs in defined B8 media [11,20]. However, its role in the adipogenic differentiation of bADSCs has not been examined. Based on these observations, we hypothesized that albumin supports adipogenic differentiation under serum-free conditions. To test this hypothesis, bADSCs isolated from adipose tissue (Fig. 1A) were cultured in B8 medium supplemented with 10 mg mL^{-1} albumin, the most effective concentration for bMuSC culture [20]. A 3% FBS-based adipogenic differentiation medium was used as a serum-containing comparator, as previously described for bovine adipogenesis [26]. Strikingly, lipid droplet formation was observed on day 2, markedly earlier than under conventional FBS-based conditions. Albumin supplementation resulted in up to a 31.5-fold increase in ORO-positive area compared with FBS-based conditions. Reducing albumin concentration proportionally decreased lipid accumulation, indicating a dose-dependent effect (Fig. 1B–D).

Consistent with these findings, the expression of adipogenic markers (FABP4, LPL, ADIPOQ, and PPARG) was upregulated with increasing albumin concentrations, whereas that of anti-adipogenic markers (DLK1, KLF2, and WNT10B) was downregulated (Fig. 1E). Based on these results, 10 mg mL^{-1} albumin was used in subsequent experiments.

Time-course gene expression analysis further showed sequential changes in adipogenic marker expression following albumin supplementation. Early, intermediate, and late adipogenic markers were upregulated on days 2–4, around day 6, and after day 8, respectively (Fig. 1F). This temporal expression pattern is consistent with the early onset of lipid accumulation observed on day 2. In contrast, these temporal expression patterns were markedly attenuated in the absence of albumin.

Collectively, these results show that albumin supplementation supports early lipid accumulation and adipogenic marker expression under serum-free conditions.

Adipogenic differentiation condition optimization

We evaluated the effects of conventional adipogenic inducers on adipogenic differentiation under albumin-based conditions. Supplementation with ROSI, with or without IND, resulted in up to a 3.9-fold increase in ORO-positive area compared to B8 + albumin conditions (Fig. 2A, B). In contrast, the commonly used inducers IBMX and DEX reduced lipid accumulation. Consistently, the expression of adipogenic markers (FABP4 and PPARG) was significantly upregulated under the ROSI and ROSI + IND conditions (Fig. 2C). Although both conditions increased lipid accumulation and adipogenic marker expression, ROSI alone was selected for subsequent formulation optimization.

Component-dropout analysis identifies key factors for adipogenesis

To identify the components required to support adipogenic differentiation, we performed component-dropout analysis under albumin-based serum-free conditions. The partial or complete removal of individual components revealed that most factors had a limited impact. However, ROSI, INS, or L-ascorbic acid removal markedly reduced lipid accumulation. In addition, even 50% bFGF reduction significantly reduced lipid accumulation, indicating a dose-dependent response to bFGF (Fig. 3A). Gene expression analysis supported these findings, as ROSI, INS, or bFGF removal significantly downregulated adipogenic marker expression (Fig. 3B). In contrast, transforming growth factor beta 3 (TGFβ3) removal increased adipogenic marker expression, indicating that TGFβ3 was not required under these conditions.

Based on these results, a reduced-component adipogenic differentiation medium consisting of albumin, ROSI, INS, bFGF, and L-ascorbic acid was defined and designated as ‘AdB5.’ AdB5 supported adipogenic differentiation comparable to the B8 + albumin + ROSI conditions, with similar lipid accumulation (Fig. 3C, D). FABP4 expression was higher in the AdB5 condition, whereas PPARG expression was higher in the B8 + albumin + ROSI condition (Fig. 3E).

To further optimize basal conditions, we compared multiple media formulations. DMEM/F12 and DMEM showed similar lipid accumulation, whereas αMEM and Advanced MEM showed lower lipid accumulation (fig. S1A). Based on these results, the DMEM/F12-based AdB5 medium was selected for subsequent experiments. Increasing the albumin concentration above 10 mg mL^{-1} did not further increase lipid accumulation (fig. S1B). Extending differentiation to 20 days further increased lipid accumulation, with greater lipid accumulation than that observed on day 10 (fig. S1C). Notably, AdB5 showed up to a 65.1-fold higher ORO-positive area than the FBS-based condition (fig. S1D).

AdB5 was further evaluated in bADSCs derived from an independent donor (fig. S2A). BODIPY and ORO staining showed increased lipid accumulation under AdB5 conditions compared with FBS-based conditions (fig. S2B–E). Adipogenic markers were also upregulated, and anti-adipogenic markers were downregulated (fig. S2F). Together, these results show that AdB5 also supports adipogenic differentiation in bADSCs from an independent donor.

Fig. S2. Validation of AdB5 differentiation medium in an additional cell line. (A) Mean gene expression changes in bovine adipose-derived stem cells measured by RT-qPCR were compared with those in bovine muscle stem cells. Error bars indicate standard error of the mean (SEM), n = 3. (***$p < 0.001$). **(B)** Representative bright-field images showing the morphological differences between the 3% FBS and AdB5 conditions. Scale bar, 200 μm. **(C)** Representative fluorescence images of ADSCs cultured in 3% FBS and AdB5. Green, BODIPY; blue, DAPI. Scale bar, 200 μm. **(D)** Representative Oil Red O-stained images of ADSCs in 3% FBS and AdB5 conditions. Scale bar, 200 μm. **(E)** Quantification of Oil Red O-positive area corresponding to **(D)**; error bars indicate SEM, n = 6. (***$p < 0.001$). **(F)** Mean adipogenic marker gene expression changes in the 3% FBS and AdB5 conditions, as determined by RT-qPCR; error bars indicate SEM, n = 3.

Adipogenic–myogenic co-differentiation under AdB5 conditions

Coordinated adipocyte and myocyte differentiation is required to reproduce the structural and sensory properties of conventional meat [3,5]. Therefore, we first assessed whether AdB5 supports myogenic differentiation. bMuSCs were differentiated in AdB5 or and FBS-based muscle differentiation medium containing 2% FBS for 3 days [27,28]. Immunostaining for the myosin heavy chain (MyHC) showed extensive myotube formation under AdB5 conditions (Fig. 4A). The fusion index reached 47.2% in AdB5 cells (Fig. 4B).

Next, we evaluated adipogenic–myogenic co-differentiation. bADSCs and bMuSCs were co-cultured at defined ratios (10:0, 9:1, 7:3, 5:5, 3:7, 1:9, and 0:10) and differentiated in the AdB5 medium. Lipid accumulation (BODIPY) was minimal when the bADSC ratio was ≤ 30%, whereas MyHC expression was significantly reduced when the bMuSC ratio was ≤ 10% (Fig. 4C). Both adipogenic and myogenic phenotypes were observed at intermediate ratios (5:5 and 7:3). Gene expression analysis supported these phenotypes. Myogenic markers increased in cultures containing ≥ 70% bMuSCs, whereas adipogenic markers were the highest in cultures containing ≥ 90% bADSCs (Fig. 4D). Together, these results show that intermediate bADSC-bMuSC ratios support both adipogenic and myogenic differentiation under a single AdB5 condition.

AdB5 supports adipogenic–myogenic co-differentiation in 3D scaffold systems

We evaluated the performance of AdB5 in 3D cultures using gelatin methacrylate (GelMA) cryogels scaffold (Fig. 5A, B). GelMA supported uniform and robust lipid accumulation throughout the scaffold (Fig. 5C–E). Next, we assessed myogenic differentiation within GelMA. The bMuSCs cultured in AdB5 formed well-organized MyHC-positive myotubes throughout the scaffold, confirming that GelMA supported efficient myogenic differentiation in the 3D environment (Fig. 5F). Subsequently, co-differentiation was evaluated using GelMA. Adipocytes and myotubes were simultaneously observed within a single scaffold under AdB5 conditions, demonstrating coordinated adipogenic–myogenic

differentiation in 3D culture (Fig. 5G). Taken together, these results demonstrate that the combination of AdB5 and GelMA supports the formation of composite muscle–adipose structures relevant to structured meat production.

AdB5 induces distinct early adipogenic transcriptional responses

To characterize the early adipogenic response under AdB5, we performed RNA sequencing on days 2 and 4 under GM-, AdB5-, and FBS-based differentiation conditions. Correlation analysis and hierarchical clustering separated samples by condition, with AdB5-treated samples forming a distinct cluster, whereas FBS-treated samples remained closer to the GM-treated samples, showing greater transcriptional similarity between the FBS and GM conditions (Fig. 6A, B, S3A). Principal component analysis (PCA) further showed separation among the conditions (PC1:65.9%, PC2:20.1%) (Fig. 6C).

Differential expression analysis (DEG) revealed greater transcriptional changes with AdB5 than with FBS. Compared to GM, AdB5 upregulated 1,324 genes and downregulated 989 genes on day 2, and upregulated 1,580 and downregulated 927 genes on day 4 ($|\log2\ FC| > 1$, $FDR < 0.05$). In contrast, FBS induced fewer changes (day 2:673 upregulated, 898 downregulated; day 4:706 upregulated, 902 downregulated; Fig. 6D). Temporal analysis further showed greater transcriptional dynamics under AdB5, with 952 genes changing between days 2 and 4, compared to 238 genes under FBS conditions (Fig. 6E, F). Direct comparison between media showed further differences, with 1,283 and 1,627 upregulated genes in AdB5 on days 2 and 4, respectively (Fig. 6G).

Functional enrichment analysis showed that genes upregulated under AdB5 were strongly associated with fatty acid metabolism, beta-oxidation, extracellular matrix organization, the tricarboxylic acid (TCA) cycle, and the PPAR signaling pathway, together with innate immunity and inflammation (Fig. 6H, S3B, S3C). In contrast, FBS conditions were enriched for general cellular processes, including proliferation, apoptosis, angiogenesis, and signaling pathways such as PI3K–Akt and AMPK. These results show distinct transcriptional responses under AdB5 and FBS-based differentiation conditions.

Analysis of transcription factors on day 2 revealed upregulation of early adipogenic regulators, including CEBPB and CEBPD [29] (Fig. 6I). The expression of additional adipogenesis-associated genes (*EPAS1* [30], *VDR* [31], *XBP1* [32], *KLF11* [33], *MBD4* [34], and *NFIB* [35]) also increased. Several transcription factors not previously linked to adipogenesis, including CDIP1, ETV6, HIF1A, PKNOX2, RELB, SIX5, and STAT1, were upregulated, although their roles in adipogenic differentiation remain to be determined. The expression of AHR, a reported adipogenesis inhibitor [36], also increased, suggesting that both adipogenesis-associated and inhibitory responses occurred under AdB5 conditions. Consistent with these findings, both early and late adipogenic markers were upregulated at earlier time points under AdB5 conditions compared with FBS (Fig. 6J). Together, these results show early changes in adipogenesis-associated transcriptional programs under AdB5 conditions.

DISCUSSION

Efficient adipose tissue generation remains a major challenge in cultured meat production because adipogenic differentiation is relatively slow and often relies on serum-containing media. Furthermore, the use of FBS introduces undefined composition, batch-to-batch variability, and regulatory concerns [11,26,37]. Recent serum-free cultured meat studies have primarily focused on MuSC expansion and ADSC differentiation. Although substantial progress has been made in maintaining and expanding MuSCs under defined conditions, adipogenic differentiation remains largely dependent on serum-containing media. In addition, most adipogenesis studies have used human or rodent cells, whereas studies using livestock-derived cells remain limited [38,39].

Here, we developed AdB5 as a reduced-component, defined, serum-free system that supports rapid adipogenic differentiation of bovine ADSCs. AdB5 induced detectable lipid accumulation within 2 days, and the ORO-positive area was up to 65.1-fold higher than that observed under the FBS-based condition. AdB5 also eliminated several commonly used adipogenic inducers, including IBMX, IND, and DEX [10,40,41]. These findings show that AdB5 supports rapid lipid accumulation and adipogenic differentiation using a reduced set of components. AdB5 also supported adipogenic differentiation in bADSCs from an independent donor, although the response varied between cell lines. Further validation across additional donors will be required to assess donor-dependent variability and generalizability.

Albumin is the most abundant transport protein in serum, facilitates fatty acid transport, and stabilizes hydrophobic molecules [42]. In the AdB5 system, increasing albumin concentrations were associated with increased lipid accumulation and adipogenic marker expression. These findings suggest that albumin supports adipogenic differentiation under these conditions. Previous studies have also reported changes in albumin expression during adipocyte differentiation and its association with key adipogenic transcription factors, including PPARγ and C/EBPα [43].

Component-removal analysis showed differential responses to the removal of individual components from the AdB5 formulation. Although L-ascorbic acid removal had a limited effect on adipogenic marker expression, it reduced lipid accumulation, consistent with previous reports of its role in adipogenesis under serum-free conditions [44]. Similarly, bFGF removal reduced lipid accumulation, consistent with previous studies linking FGF/ERK signaling to adipocyte differentiation [45]. In contrast, TGFβ3 removal increased adipogenic marker expression, consistent with previous reports that TGFβ3 promotes bADSC proliferation and suppresses adipogenic differentiation through Smad3 and p38 signaling pathways [46]. Together, these results describe the responses to individual component removal within the AdB5 formulation.

Transcriptome analysis revealed early changes in adipogenesis-associated transcriptional programs following AdB5 treatment. Compared with the FBS-based condition, AdB5 induced broader transcriptional changes, including early upregulation of adipogenic regulators (PPARG, CEBP family, FABP4, ADIPOQ, and LPL), and enrichment of metabolic pathways associated with fatty acid

metabolism, beta-oxidation, the TCA cycle, and PPAR signaling [47]. In contrast, the FBS-based condition showed enrichment of signaling pathways including PI3K–Akt and AMPK. AdB5 was also associated with enrichment of innate immune and inflammatory pathways, although the functional significance of these responses remains unclear. These findings indicate distinct early transcriptional responses under AdB5 and FBS-based differentiation conditions.

Adipogenic and myogenic differentiation commonly require different culture conditions. In this study, AdB5 supported both adipogenic and myogenic differentiation under a single defined condition. Mixed bADSC-bMuSC cultures at intermediate ratios (5:5–7:3) exhibited both adipogenic and myogenic phenotypes without media switching or compartmentalization [6,48–50].

AdB5 also supported adipogenic and myogenic differentiation in 3D GelMA culture. bADSCs exhibited lipid accumulation within GelMA, while bMuSCs formed MyHC-positive myotubes. In mixed cultures, lipid-containing cells and MyHC-positive myotubes were observed within the same scaffold, showing the feasibility of adipose-muscle co-culture under AdB5 conditions in a 3D scaffold.

Despite these findings, several limitations should be considered for the translation of AdB5 to cultivated meat production. Further validation across additional donors will be required to assess generalizability. Metabolomics and lipidomic analyses may help clarify the metabolic changes associated with albumin-supported adipogenic differentiation. AdB5 should be considered an experimental defined differentiation medium rather than a production-ready food-grade medium. Rosiglitazone would require replacement with a food-compatible alternative, and bFGF may present cost and regulatory limitations. In addition, although GelMA supported 3D adipose-muscle construct formation, its direct use as an edible scaffold is limited. Future studies should therefore focus on food-compatible and cost-effective alternatives.

In summary, AdB5 is a reduced-component, serum-free, albumin-based medium that supports rapid adipogenic differentiation of bovine ADSCs. An adipogenic response was also observed in cells from an independent donor, and AdB5 supported adipogenic and myogenic differentiation in mixed bADSC-bMuSC cultures and 3D constructs. These findings provide a basis for further development of defined differentiation conditions for bovine adipose-muscle tissue engineering and cultivated meat applications.

Declarations

Ethics approval and consent to participate

Not applicable.

Consent for publication

Not applicable.

Availability of data and materials

The RNA-seq data generated in this study have been deposited in the Gene Expression Omnibus (GEO) (accession number GSE326747). The source data are provided with this study. Additional data supporting the findings of this study are available from the authors upon request. Materials used in this study are also available from the corresponding author upon reasonable request.

Competing interests

The authors declare no competing financial interests or personal relationships that could have influenced the work reported in this study.

Funding

This research was supported by Korea Institute of Planning and Evaluation for Technology in Food, Agriculture and Forestry (IPET) through the 'High Value-added Food Technology Development Program' and was funded by the Ministry of Agriculture, Food and Rural Affairs (MAFRA) (322006-05-CG000).

Authors' contributions

Y.R.K. contributed to the conceptualization and methodology of the study, performed the investigation, validation, formal analysis, and data curation, prepared the visualization, and wrote the original draft of the manuscript. S.W.J., J.H.H., G.R.N. and J.H.P contributed to methodology. S.M.P. contributed to conceptualization and administered the project. M.H.L. contributed to the conceptualization, supervised the study, administered the project, and reviewed and edited the manuscript. H.W.C. contributed to the conceptualization, supervised and administered the project, acquired funding, and reviewed and edited the manuscript.

Acknowledgements

Not applicable.

References

1. Parodi, A. *et al.* The potential of future foods for sustainable and healthy diets. *Nature Sustainability* 1, 782–789 (2018).
2. Post, M. J. *et al.* Scientific, sustainability and regulatory challenges of cultured meat. *Nature food* 1, 403–415 (2020).
3. Post, M. J. Cultured meat from stem cells: Challenges and prospects. *Meat science* 92, 297–301 (2012).
4. Frank, D., Joo, S.-T. & Warner, R. Consumer acceptability of intramuscular fat. *Korean journal for food science of animal resources* 36, 699 (2016).
5. Soleymani, S., Naghib, S. M. & Mozafari, M. An overview of cultured meat and stem cell bioprinting: How to make it, challenges and prospects, environmental effects, society's culture and the influence

of religions. *Journal of Agriculture and Food Research* 18, 101307 (2024).

6. Wang, Y., Zhuang, D., Munawar, N., Zan, L. & Zhu, J. A rich-nutritious cultured meat via bovine myocytes and adipocytes co-culture: Novel Prospect for cultured meat production techniques. *Food Chemistry* 460, 140696 (2024).
7. Lee, M. *et al.* Cultured meat with enriched organoleptic properties by regulating cell differentiation. *Nature communications* 15, 77 (2024).
8. Fish, K. D., Rubio, N. R., Stout, A. J., Yuen, J. S. & Kaplan, D. L. Prospects and challenges for cell-cultured fat as a novel food ingredient. *Trends in food science & technology* 98, 53–67 (2020).
9. Pallaoro, M. *et al.* Towards a more realistic in vitro meat: The cross talk between adipose and muscle cells. *International Journal of Molecular Sciences* 24, 6630 (2023).
10. Liu, P.-P. *et al.* Optimization of differentiation conditions for porcine adipose-derived mesenchymal stem cells and analysis of fatty acids in cultured fat. *Food Research International* 194, 114853 (2024).
11. Kim, Y. R. *et al.* Serum-free cultured meat production by using Pichia pastoris-derived recombinant albumin. *iScience* 28, 113242 (2025). https://doi.org/10.1016/j.isci.2025.113242
12. Scott, M. A., Nguyen, V. T., Levi, B. & James, A. W. Current methods of adipogenic differentiation of mesenchymal stem cells. *Stem cells and development* 20, 1793–1804 (2011).
13. Louis, F., Furuhashi, M., Yoshinuma, H., Takeuchi, S. & Matsusaki, M. Mimicking Wagyu beef fat in cultured meat: Progress in edible bovine adipose tissue production with controllable fatty acid composition. *Materials Today Bio* 21, 100720 (2023).
14. Yamanaka, K., Haraguchi, Y., Takahashi, H., Kawashima, I. & Shimizu, T. Development of serum-free and grain-derived-nutrient-free medium using microalga-derived nutrients and mammalian cell-secreted growth factors for sustainable cultured meat production. *Scientific Reports* 13, 498 (2023).
15. Messmer, T. *et al.* A serum-free media formulation for cultured meat production supports bovine satellite cell differentiation in the absence of serum starvation. *Nature Food* 3, 74–85 (2022).
16. Pasitka, L. *et al.* Spontaneous immortalization of chicken fibroblasts generates stable, high-yield cell lines for serum-free production of cultured meat. *Nature Food* 4, 35–50 (2023).
17. Chu, S. *et al.* A serum-free culture medium production system by co-culture combining growth factor-secreting cells and L-lactate-assimilating cyanobacteria for sustainable cultured meat production. *Scientific reports* 14, 19578 (2024).
18. Kolkmann, A. M., Van Essen, A., Post, M. J. & Moutsatsou, P. Development of a chemically defined medium for in vitro expansion of primary bovine satellite cells. *Frontiers in bioengineering and biotechnology* 10, 895289 (2022).
19. Schenzle, L. *et al.* Low-cost food-grade alternatives for serum albumins in FBS-free cell culture media. *Scientific Reports* 15, 15296 (2025).
20. Stout, A. J. *et al.* Simple and effective serum-free medium for sustained expansion of bovine satellite cells for cell cultured meat. *Communications Biology* 5, 466 (2022).

21. Mitić, R., Cantoni, F., Börlin, C. S., Post, M. J. & Jackisch, L. A simplified and defined serum-free medium for cultivating fat across species. *IScience* 26 (2023).
22. Klatt, A. *et al.* Dynamically cultured, differentiated bovine adipose-derived stem cell spheroids as building blocks for biofabricating cultured fat. *Nature communications* 15, 9107 (2024).
23. Xuan, Z. *et al.* Development of a sustainable strategy for cultured fat production based on serum-free 3D culture of bovine adipose stem cells. *Scientific Reports* 15, 44793 (2025).
24. Shirahama, H., Lee, B. H., Tan, L. P. & Cho, N. J. Precise Tuning of Facile One-Pot Gelatin Methacryloyl (GelMA) Synthesis. *Sci Rep* 6, 31036 (2016). https://doi.org/10.1038/srep31036
25. Ma, C. *et al.* Mammalian and Fish Gelatin Methacryloyl-Alginate Interpenetrating Polymer Network Hydrogels for Tissue Engineering. *ACS Omega* 6, 17433–17441 (2021). https://doi.org/10.1021/acsomega.1c01806
26. Mitić, R., Cantoni, F., Börlin, C. S., Post, M. J. & Jackisch, L. A simplified and defined serum-free medium for cultivating fat across species. *iScience* 26, 105822 (2023). https://doi.org/10.1016/j.isci.2022.105822
27. Messmer, T. *et al.* A serum-free media formulation for cultured meat production supports bovine satellite cell differentiation in the absence of serum starvation. *Nat Food* 3, 74–85 (2022). https://doi.org/10.1038/s43016-021-00419-1
28. Ding, S. *et al.* Maintaining bovine satellite cells stemness through p38 pathway. *Sci Rep* 8, 10808 (2018). https://doi.org/10.1038/s41598-018-28746-7
29. Tang, Q.-Q. & Lane, M. D. Activation and centromeric localization of CCAAT/enhancer-binding proteins during the mitotic clonal expansion of adipocyte differentiation. *Genes & development* 13, 2231–2241 (1999).
30. Shimba, S., Wada, T., Hara, S. & Tezuka, M. EPAS1 promotes adipose differentiation in 3T3-L1 cells. *Journal of Biological Chemistry* 279, 40946–40953 (2004).
31. Blumberg, J. M. *et al.* Complex role of the vitamin D receptor and its ligand in adipogenesis in 3T3-L1 cells. *Journal of Biological Chemistry* 281, 11205–11213 (2006).
32. Sha, H. *et al.* The IRE1α-XBP1 pathway of the unfolded protein response is required for adipogenesis. *Cell metabolism* 9, 556–564 (2009).
33. Yamamoto, K.-i. *et al.* Transcriptional regulation of a brown adipocyte-specific gene, UCP1, by KLF11 and KLF15. *Biochemical and biophysical research communications* 400, 175–180 (2010).
34. Zhang, L.-J. *et al.* The MBD4 gene plays an important role in porcine adipocyte differentiation. *Cellular Physiology and Biochemistry* 34, 1216–1226 (2014).
35. Waki, H. *et al.* Global mapping of cell type–specific open chromatin by FAIRE-seq reveals the regulatory role of the NFI family in adipocyte differentiation. *PLoS genetics* 7, e1002311 (2011).
36. Shimba, S., Wada, T. & Tezuka, M. Arylhydrocarbon receptor (AhR) is involved in negative regulation of adipose differentiation in 3T3-L1 cells: AhR inhibits adipose differentiation independently of dioxin. *Journal of cell science* 114, 2809–2817 (2001).

37. Lee, Y. S., Lee, H. J. & Jo, C. Integrative Adipogenic Engineering of Cultured Fat for Cell Based Meat. *Compr Rev Food Sci Food Saf* 25, e70338 (2026). https://doi.org/10.1111/1541-4337.70338
38. Sugii, S., Wong, C. Y. Q., Lwin, A. K. O. & Chew, L. J. M. Reassessment of adipocyte technology for cellular agriculture of alternative fat. *Comprehensive reviews in food science and food safety* 21, 4146–4163 (2022).
39. Dufau, J. *et al.* In vitro and ex vivo models of adipocytes. *American Journal of Physiology-Cell Physiology* 320, C822–C841 (2021).
40. Xuan, Z. *et al.* Development of a sustainable strategy for cultured fat production based on serum-free 3D culture of bovine adipose stem cells. *Sci Rep* 15, 44793 (2025). https://doi.org/10.1038/s41598-025-28441-4
41. Boone, C., Gregoire, F. & Remacle, C. Culture of porcine stromal-vascular cells in serum-free medium: differential action of various hormonal agents on adipose conversion. *Journal of animal science* 78, 885–895 (2000).
42. van der Vusse, G. J. Albumin as fatty acid transporter. *Drug metabolism and pharmacokinetics* 24, 300–307 (2009).
43. Yoo, W. *et al.* Albumin expression is required for adipocyte differentiation of 3T3-L1 cells. *Biochemical and biophysical research communications* 397, 170–175 (2010).
44. Jurek, S. *et al.* Optimizing adipogenic transdifferentiation of bovine mesenchymal stem cells: a prominent role of ascorbic acid in FABP4 induction. *Adipocyte* 9, 35–50 (2020).
45. Donzelli, E. *et al.* ERK1 and ERK2 are involved in recruitment and maturation of human mesenchymal stem cells induced to adipogenic differentiation. *Journal of Molecular Cell Biology* 3, 123–131 (2011).
46. Yang, L. *et al.* TGFβ3 regulates adipogenesis of bovine subcutaneous preadipocytes via typical Smad and atypical MAPK signaling pathways. *Electronic Journal of Biotechnology* 61, 33–44 (2023).
47. Sugii, S., Wong, C. Y. Q., Lwin, A. K. O. & Chew, L. J. M. Alternative fat: redefining adipocytes for biomanufacturing cultivated meat. *Trends in biotechnology* 41, 686–700 (2023).
48. Li, A. *et al.* Effect of neudesin neurotrophic factor on differentiation of bovine preadipocytes and myoblasts in a co-culture system. *Animals* 11, 34 (2020).
49. Cui, H. *et al.* Method using a co-culture system with high-purity intramuscular preadipocytes and satellite cells from chicken pectoralis major muscle. *Poultry science* 97, 3691–3697 (2018).
50. Kang, D.-H. *et al.* Engineered whole cut meat-like tissue by the assembly of cell fibers using tendon-gel integrated bioprinting. *Nature communications* 12, 5059 (2021).

Figures

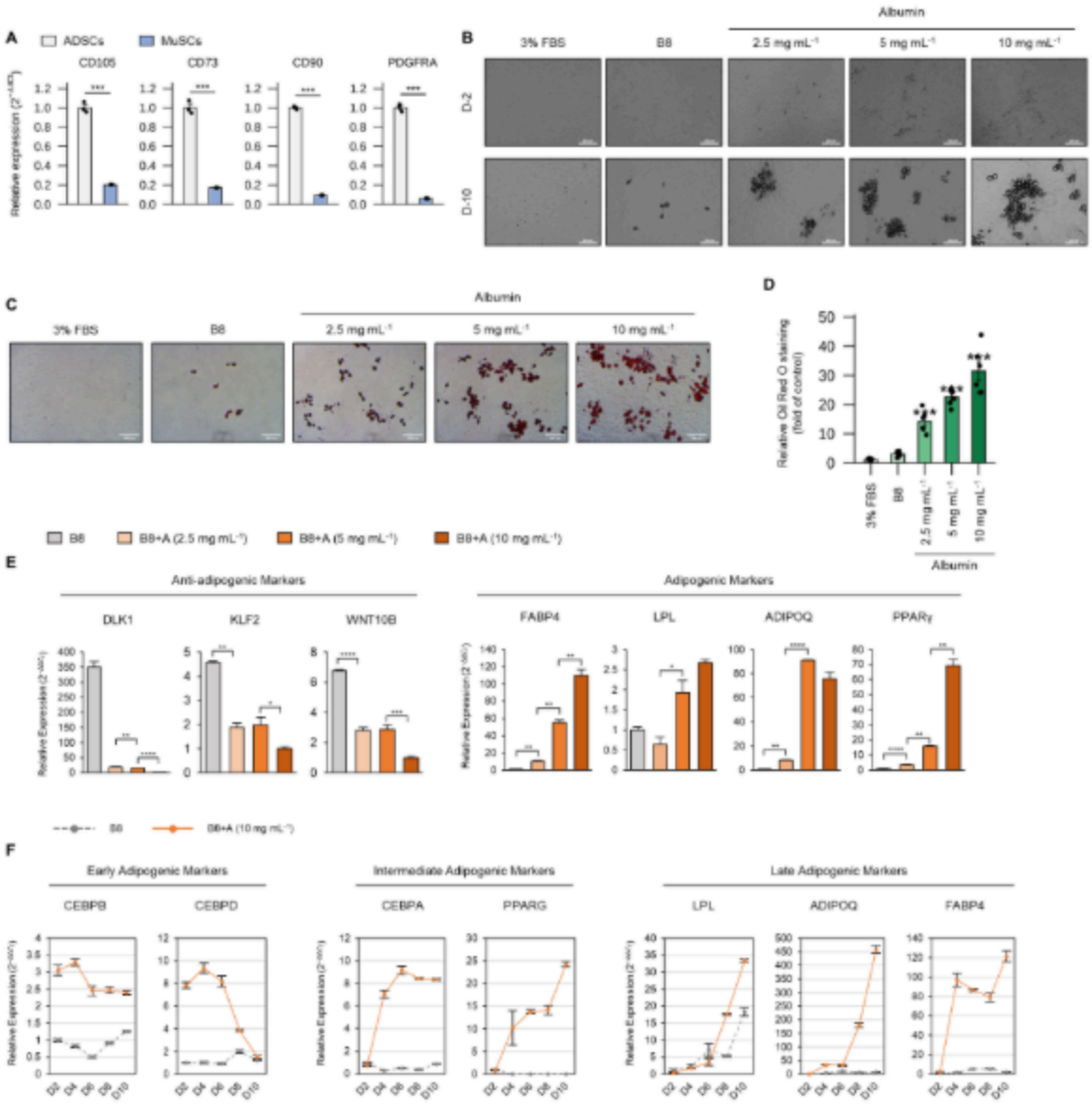


Figure 1

Albumin promotes the adipogenesis of bovine adipose-derived stem cells. (A) Mean gene expression changes in bovine ADSCs measured by RT-qPCR were compared with those in bovine muscle stem cells. Error bars indicate standard error of the mean (SEM), n=3. **(B)** Representative bright-field images showing morphological changes during adipogenic differentiation on days 2 and 10. Scale bar, 200 mm. **(C)** Representative Oil Red O-stained images of ADSCs differentiated under 3% fetal bovine serum (FBS) and B8 + varying concentrations of albumin supplementation. Scale bar, 200 mm. **(D)** Oil Red O-positive area quantification corresponding to c; error bars indicate SEM, n=6. (***p<0.001). **(E)** Mean adipogenic marker gene expression changes according to albumin concentration, determined by RT-qPCR; error bars indicate SEM, n=3. **(F)**Mean adipogenic marker gene expression changes over time, determined by RT-qPCR; error bars indicate SEM, n=3.

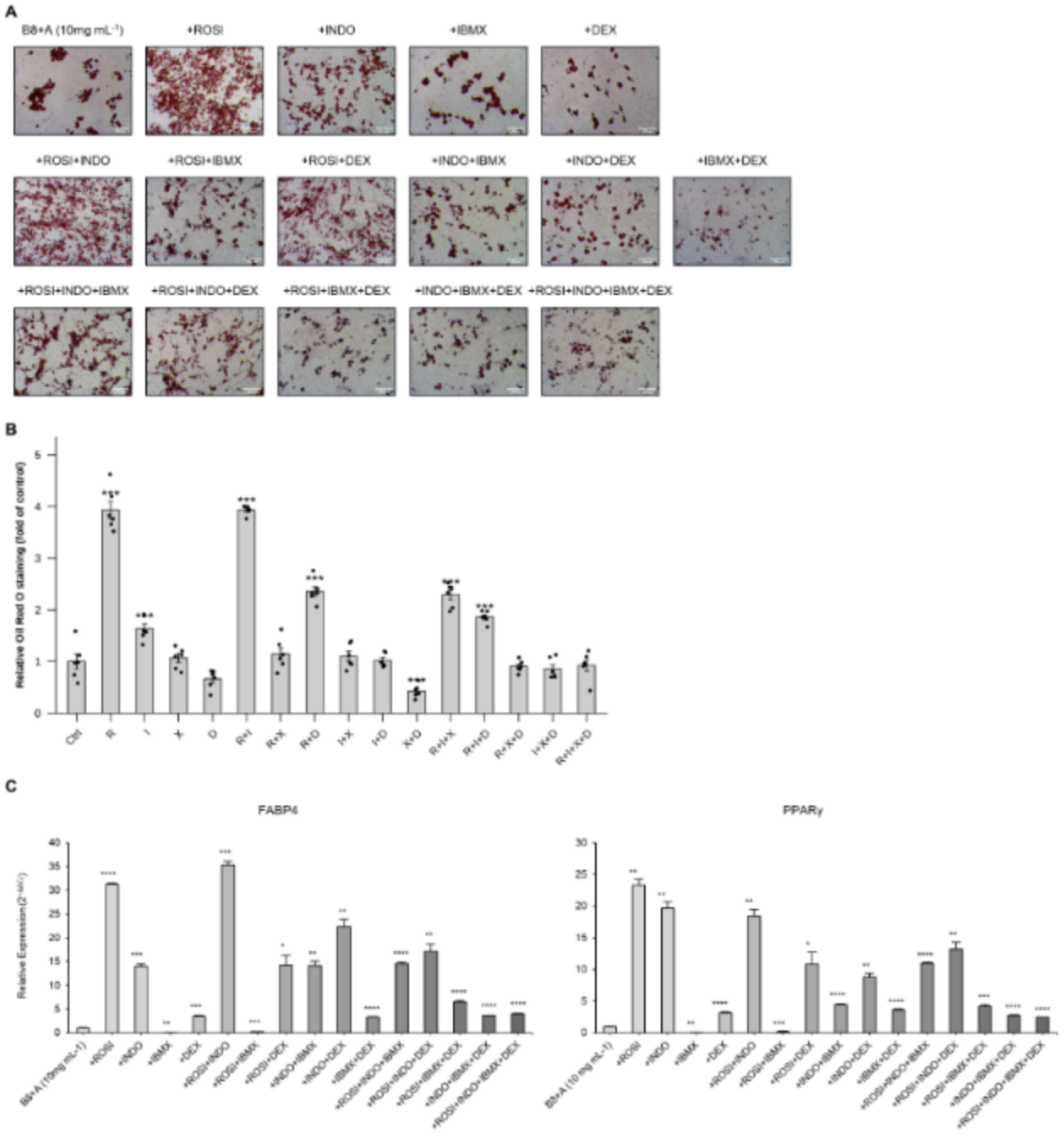


Figure 2

Identification of the optimal adipogenic inducer cocktails. (A) Representative Oil Red O-stained images of adipose-derived stem cells (ADSCs) differentiated under various adipogenic supplements. B8 + 10 mg mL^{-1} albumin is control condition. Supplements are abbreviated as 'ROSI' (rosiglitazone), 'INDO' (indomethacin), 'DEX' (dexamethasone), and 'IBMX' (3-isobutyl-1-methylxanthine). Scale bar, 200 mm. **(B)** Oil Red O-positive area quantification corresponding to a. Supplements are abbreviated as 'R' (rosiglitazone), 'I' (indomethacin), 'D' (dexamethasone), and 'X' (3-isobutyl-1-methylxanthine); error bars indicate standard error of the mean (SEM), n=6. (***p<0.001). **(**B) Mean adipogenic marker gene expression changes according to adipogenic inducer combination, determined by RT-qPCR; error bars indicate SEM, n=3.

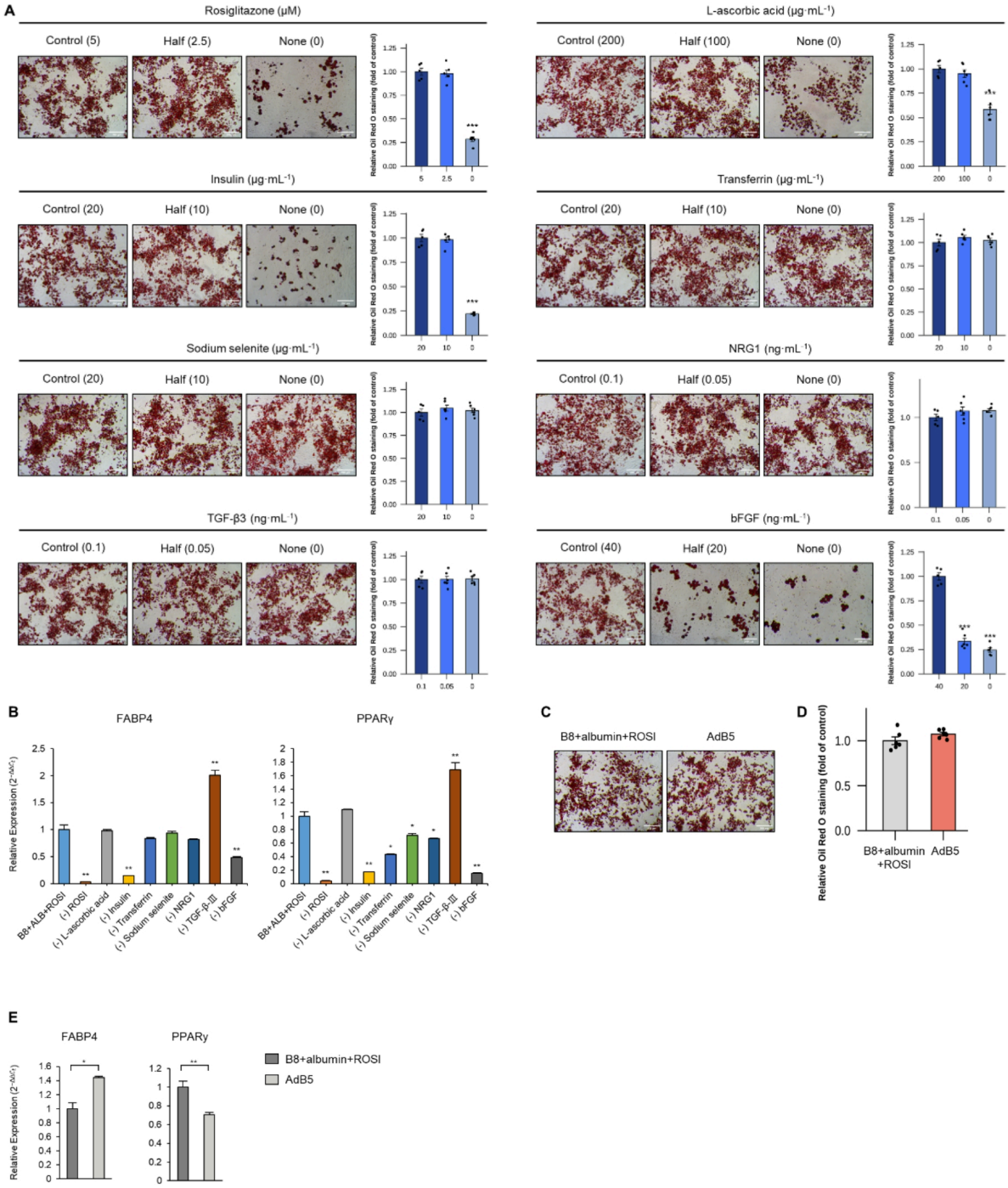


Figure 3

Component-dropout analysis to identify key adipogenic factors. (A) Representative Oil Red O-stained images (Scale bar, 200 mm) and quantification of Oil Red O-positive area in adipose-derived stem cells (ADSCs) differentiated under component-dropout conditions. B8 + 10 mg mL^{-1} albumin + Rosiglitazone is control condition; error bars indicate standard error of the mean (SEM), n=6. (***p<0.001). **(B)** Mean adipogenic marker gene expression changes following component removal, determined by RT-qPCR;

error bars indicate SEM, n=3. **(C)** Representative Oil Red O-stained images of ADSCs differentiated under B8 + 10 mg mL^{-1} albumin + Rosiglitazone and AdB5 condition. Supplements are abbreviated as 'ROSI' (rosiglitazone). Scale bar, 200 mm. **(D)** Oil Red O-positive area quantification corresponding to c; error bars indicate SEM, n=6. **(E)** Mean gene expression changes of adipogenic markers in B8 + albumin + rosiglitazone and AdB5 condition, determined by RT-qPCR; error bars indicate SEM, n=3.

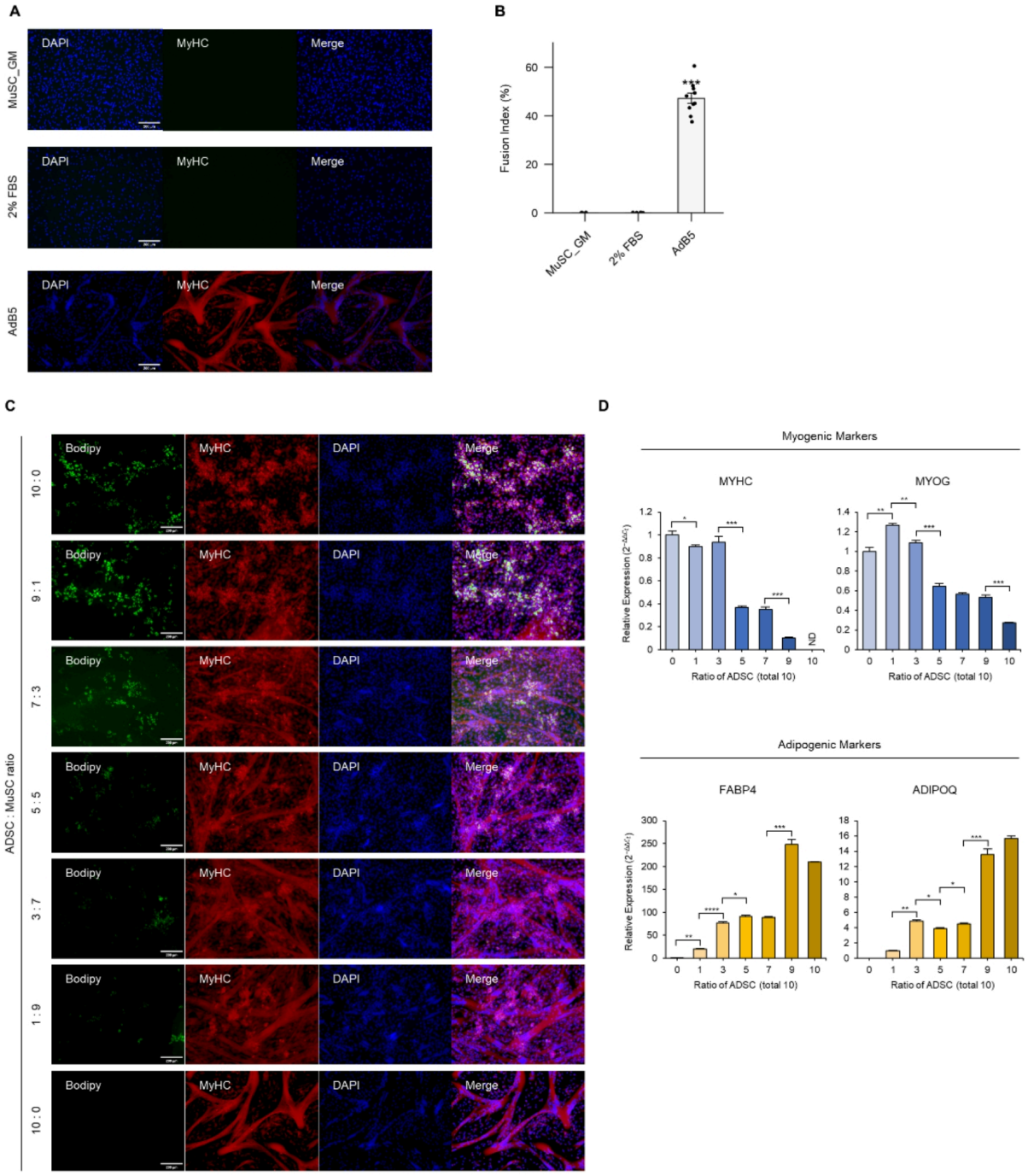


Figure 4

Adipogenic–myogenic co-differentiation under AdB5 conditions. (A) Representative fluorescence images of MuSCs under GM, 2% fetal bovine serum (FBS), and AdB5 conditions. Red, MyHC; blue, DAPI. Scale bar, 200 mm. **(B)** Fusion index corresponding to a; error bars indicate standard error of the mean (SEM), n=10. (***p<0.001). **(C)** Representative fluorescence images of ADSCs and MuSCs co-differentiated at various cell ratios. Red, MyHC; green, BODIPY; blue, DAPI. Scale bar, 200 mm. **(D)** Mean gene expression changes of adipogenic markers and myogenic markers according to cell ratio, determined by RT-qPCR; error bars indicate SEM, n=3.

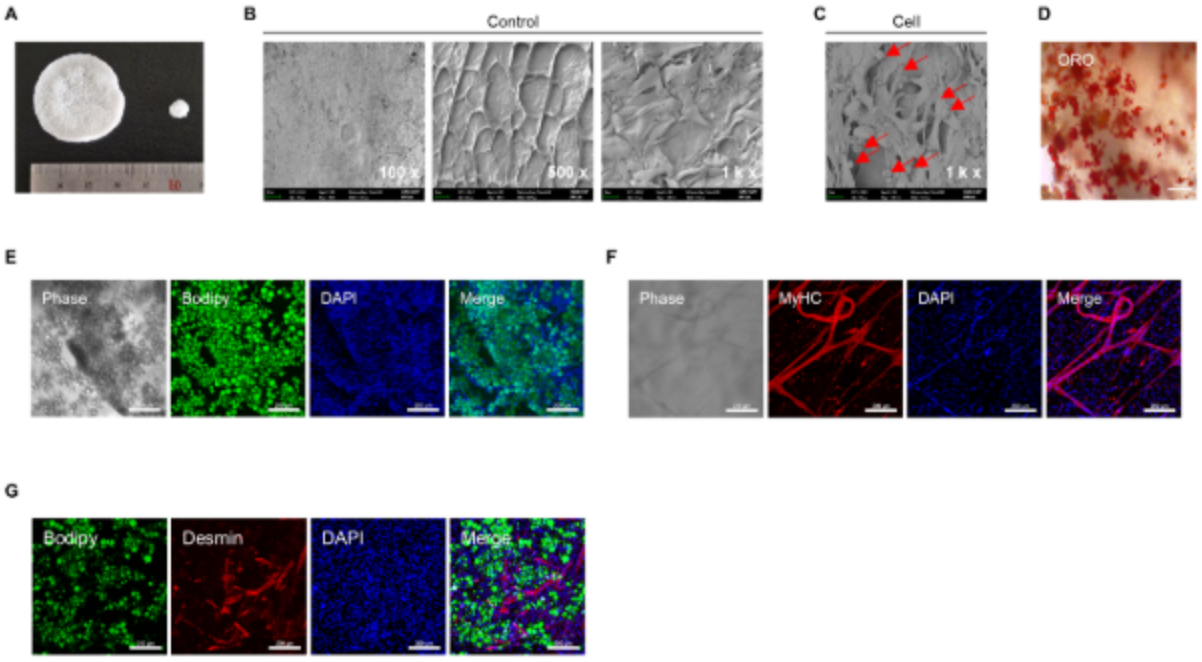


Figure 5

Evaluation of adipogenic differentiation efficiency of AdB5 under 3D scaffold culture conditions. (A) Macroscopic morphology of GelMA cryogels (left: 3.5 cm; right: 96-well), with a ruler for scale. **(B)** Representative scanning electron microscopy images of GelMA scaffolds without cells at 100×, 500×, and 1k× magnification. **(C)** Representative scanning electron microscopy images of GelMA scaffolds with adipose-derived stem cells at 1k× magnification. **(D)**Representative Oil Red O-stained images of ADSCs cultured in GelMA scaffolds under AdB5 condition. Scale bar, 200 mm. **(E)** Representative fluorescence and bright-field images of ADSCs cultured in GelMA scaffolds under AdB5 condition. Green, BODIPY; blue, DAPI. Scale bar, 200 mm. **(F)** Representative fluorescence and bright-field images of MuSCs cultured in GelMA scaffolds under AdB5 condition. Red, MyHC; blue, DAPI. Scale bar, 200 mm. **(G)**Representative fluorescence and bright-field images of MuSCs cultured in GelMA scaffolds under AdB5 condition. Red, MyHC; blue, DAPI. Scale bar, 200 mm.

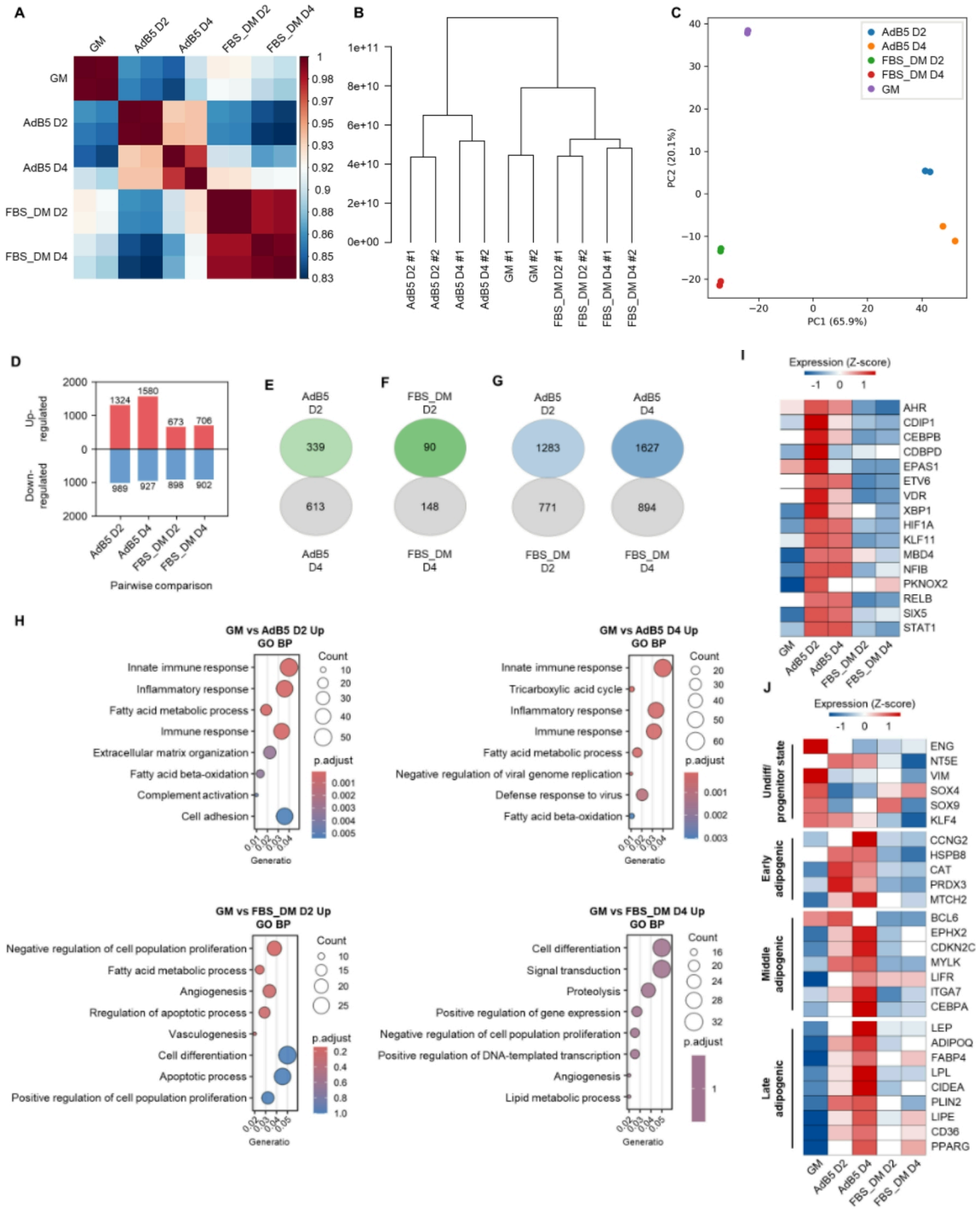


Figure 6

Transcriptomic analysis reveals accelerated early adipogenic differentiation under AdB5 condition. **(A)**Sample-to-sample correlation analysis of RNA-seq data across the GM, AdB5_D2, AdB5_D4, FBS_DM_D2, and FBS_DM_D4 conditions. **(B)** Hierarchical clustering of global gene expression profiles showing sample segregation by differentiation conditions and time points. **(C)** Principal component analysis of transcriptomic profiles showing distinct clustering of AdB5-treated samples from FBS_DM

and GM groups. **(D)** Number of differentially expressed genes (DEGs) in each condition compared to GM. **(E)** Number of DEGs between days 2 and day 4 within AdB5. **(F)** Number of DEGs between days 2 and day 4 within FBS_DM. **(G)** Number of DEGs between AdB5 and FBS_DM at days 2 and 4. **(H)** Gene ontology enrichment analysis of DEGs in each condition compared to GM. **(I)**Heatmap of differentially expressed transcription factors at AdB5 day 2. **(J)** Heatmap of DEGs associated with adipogenic regulation.

Supplementary Files

This is a list of supplementary files associated with this preprint. Click to download.

- SuppTablesandFigs.docx